DALTON

Heteroleptic poly(pyrazolyl)borate derivatives of the lanthanides. Structural and electronic spectral studies of some salicylaldehyde complexes †

Royston G. Lawrence,[a] Christopher J. Jones *[,a] and Roman A. Kresinski[b]

[a] *School of Chemistry, The University of Birmingham, Birmingham B15 2TT, UK*
[b] *School of Sciences, Staffordshire University, College Road, Stoke-on-Trent, Staffordshire ST4 2DE, UK*

The new complexes $[Ln\{HB(pz)_3\}_2L]$ [pz = pyrazol-1-yl; L = salicylaldehydate, Ln = Y, Pr, Nd, Sm, Eu, Gd, Tb, Dy, Ho, Er, Yb or Lu; L = 5-methoxysalicylaldehydate (mosal), Ln = Y, Pr, Nd, Sm, Eu, Gd, Tb, Yb or Lu] have been synthesised and the crystal structure of $[Eu\{HB(pz)_3\}_2(mosal)]$ determined. The europium ion is eight-co-ordinate with Eu–O distances of 2.266(5) and 2.402(5) Å; polytopal analysis indicates that the co-ordination geometry is best described as dodecahedral. The solid-angle sum of 0.768 is close to the norm for eight-co-ordination. These structural parameters were compared with those calculated for the previously reported binuclear complex $[\{Sm[HB(pz)_3]\}_2(O_2CPh)\}_2]$ and estimated for its monomeric counterpart, which is as yet unknown. The use of such data in predicting when complexes of this type will dimerise was assessed. Electronic spectra of the neodymium complexes revealed less than 1% covalency in the metal–ligand bonding and emission spectral data are reported for the europium and terbium complexes.

Co-ordination complexes of the lanthanide ions offer an opportunity, rare in the Periodic Table of elements, to study the stereochemistry of the ligands in the near total absence of covalent metal–ligand interactions.[1] The lack of appreciable d- or f-orbital influence on the metal–ligand bonding, coupled with the smooth variation of ionic radii available by appropriate choice of lanthanide, have made it possible to investigate the variation in co-ordination geometry and steric saturation in a series of complexes which differ only in the radius of the central metal ion.[2]

One series of compounds which is amenable to such studies is provided by the heteroleptic complexes $[Ln\{HB(pz)_3\}_2X]$ [$Ln^{3+} = Y^{3+}$ or a trivalent lanthanide ion; pz = pyrazol-1-yl, $X^- = HB(pz)_3^-$ β-diketonate, tropolonate (tropolone = 2-hydroxycyclohepta-2,4,6-trien-1-one) or carboxylate][3–7] which are unexpectedly stable towards disproportionation.[8] In the case of β-diketonate coligands, soluble monomeric complexes may be isolated for the full range of lanthanide ions from La^{3+} to Lu^{3+}. However, with the smaller carboxylate ligands monomeric complexes have only been observed for the smaller lanthanide ions. Thus in the case of Sm^{3+} the binuclear complex $[\{Sm[HB(pz)_3]\}_2(O_2CPh)\}_2]$ has been structurally characterised in the solid state,[9] whilst $[Yb\{HB(pz)_3\}_2(O_2CPh)]$ is monomeric in the solid state.[7] This finding reflects the extent to which the coligand X is able sterically to saturate the $Ln[HB(pz)_3]_2^+$ unit. The smaller carboxylate ligands appear less able than β-diketonates to saturate the lanthanide co-ordination sphere in the larger lanthanide ions. Thus stable monomeric complexes of formula $[Ln\{HB(pz)_3\}_2(O_2CPh)]$ form over a narrower range of lanthanide ion radii.

The degree of steric crowding in a lanthanide complex can be estimated by means of solid-angle factor (s.a.f.) and solid-angle sum (s.a.s.) calculations.[2] Respectively, these represent the fraction of co-ordination space occupied by a ligand bonded to a lanthanide ion and that occupied by all of the ligands. In this paper we report the first structural study of a monomeric complex of general formula $[Ln\{HB(pz)_3\}_2X]$ involving a 'middle-sized' lanthanide ion, Eu^{3+}, and of a salicylaldehyde derivative co-ordinated to Eu^{3+}. The application of the concept of steric angle sum in rationalising the formation of a monomeric structure by Eu^{3+} in $[Eu\{HB(pz)_3\}_2(mosal)]$ (Hmosal = 5-methoxysalicylaldehyde) and a binuclear structure by the similarly sized Sm^{3+} in $[\{Sm[HB(pz)_3]\}_2(O_2CPh)\}_2]$ is examined.

Results and Discussion

Synthetic studies

The new heteroleptic complexes $[Ln\{HB(pz)_3\}_2(sal)]$ (Ln = Y, Pr, Nd, Sm, Eu, Gd, Tb, Dy, Ho, Er, Yb or Lu; Hsal = salicylaldehyde) and $[Ln\{HB(pz)_3\}_2(mosal)]$ (Ln = Y, Pr, Nd, Sm, Eu, Gd, Tb, Yb or Lu) were precipitated from alkaline aqueous ethanol media in a reaction between $K[HB(pz)_3]$, Hsal or Hmosal and a salt of yttrium or the appropriate lanthanide in the mole ratio 2:1:1. The products obtained were dried and purified by recrystallisation from CH_2Cl_2–hexane mixtures. Reactions carried out with La^{3+} or Ce^{3+} afforded materials insoluble in polar organic solvents, a finding which contrasts with the production of the soluble complexes $[Ln\{HB(pz)_3\}_2(acac)]$ [Ln = La or Ce; acac = MeC(O)CHC(Me)O].[6] Elemental analyses of the new complexes (Table 1) were generally in accord with expectation but in a few cases those for carbon were lower than expected by between 0.5 and 1.4% despite repeated recrystallisations. Thermogravimetric analyses of these compounds provided no evidence for the presence of volatile contaminants such as water or pyrazole and it is possible that these samples were contaminated with a small proportion of $[Ln\{HB(pz)_3\}_3]$, possibly as a result of some disproportionation during recrystallisation.

The IR spectra (Table 1) of the new complexes all exhibit bands consistent with the presence of the ligand $HB(pz)_3$ including ν_{BH} in the range 2440–2480 cm^{-1}. In the cases of $[Ln\{HB(pz)_3\}_2(mosal)]$ (Ln = Y, Eu, Tb, Yb or Lu) the solid-state spectra contain two bands in the regions 2473–2476 and 2444–2446 cm^{-1}. However, solution spectra (CCl_4) contain only one band in the region 2454–2456 cm^{-1} indicating that this is a solid-state effect as has been observed previously for $[Ln\{HB(pz)_3\}_2(O_2CPh)]$ (Ln = Y, Yb or Lu).[7] A band is

† *Supplementary data available* (No. SUP 57122, 4 pp.): electronic spectral data.
Non-SI unit employed: $\mu_B \approx 9.27 \times 10^{-24}$ J T^{-1}.

Table 1 Characterisation data for $[Ln\{HB(pz)_3\}_2(sal)]$ and $[Ln\{HB(pz)_3\}_2(mosal)]$

Ln	M.p./°C	Analysis (%) C	H	N	IR (cm^{-1})[a] ν(BH)	ν(CO)	^1H NMR[b] (δ) Pyrazolyl			Aryl and methoxy				CHO	Mass spectrum (m/z for M^+)[c]
$[Ln\{HB(pz)_3\}_2(sal)]$															
Y	210	46.1 (47.2)	4.1 (4.0)	26.6 (26.4)	2462	1629	9.38	7.62	7.06	5.95	7.40	6.69	6.55	9.38	635 (636)
Pr	225	43.1 (43.6)	3.7 (3.7)	23.9 (24.4)	2465	1622	10.13	6.76	5.54	30.64	26.80	26.53	21.38	44.10	687 (688)
Nd	219	42.9 (43.4)	3.6 (3.7)	24.3 (24.3)	2466	1622	9.72	7.35	4.90	22.28	16.72	15.50	12.97	25.49	689 (689)
Sm	221	42.4 (43.1)	3.9 (3.6)	24.3 (24.1)	2467	1623	8.41	5.85	4.46	8.81	8.22	7.80	7.65	8.92	699 (698)
Eu	218	43.3 (43.0)	3.5 (3.6)	24.2 (24.0)	2468	1623	10.87	3.46	2.86	1.68	0.92	−2.29	−6.72	−15.52	700 (699)
Gd	225	41.9 (42.6)	3.8 (3.6)	23.5 (23.9)	2468	1624									705 (704)
Tb	224	42.2 (42.5)	3.5 (3.6)	23.6 (23.8)	2468	1624									705 (706)
Dy	214	42.2 (42.3)	3.7 (3.6)	23.5 (23.7)	2468	1626	21.11	−1.85	−34.15	178.22	148.13	−75.25	−75.25	181.16	709 (710)
Ho	221	41.3 (42.2)	3.5 (3.5)	22.8 (23.6)	2468	1626	1.42	0.61	−23.05	74.74	72.83	62.35	−3.71	146.1	711 (712)
Er	220	41.7 (42.0)	3.9 (3.5)	23.4 (23.5)	2468	1626	48.23	5.07	−4.93	−28.28	−30.36	−36.44	−38.57	−50.48	714 (713)
Yb	209	41.3 (41.7)	3.6 (3.5)	23.2 (23.3)	2468	1628	23.04	6.30	4.76	13.79	−11.09	−12.18	−15.98	−45.00	653[d] (720)
Lu	214	41.1 (41.6)	3.2 (3.5)	23.0 (23.3)	2467	1627	7.63	7.06	5.95	7.41	6.70	6.57	9.39		721 (722)
$[Ln\{HB(pz)_3\}_2(mosal)]$													OCH_3		
Y	204	45.5 (46.9)	4.0 (4.1)	24.8 (25.2)	2457	1637	7.63	7.06	5.96	7.14	6.76	6.68	3.77	9.33	665 (666)
Pr	205	43.5 (43.5)	3.7 (3.8)	23.8 (23.4)	2473 2444	1637	10.20	6.76	5.50	30.83	26.59	25.90	11.92	44.42	717 (717)
Nd	202	43.5 (43.5)	3.7 (3.8)	23.6 (23.3)	2473 2444	1638	0.12	−2.32	−6.00	15.55	9.40	7.79	2.44	18.55	718 (718)
Sm	201	42.5 (42.9)	4.0 (3.7)	23.1 (23.1)	2475 2445	1640	8.41	5.85	4.43	8.21	7.96	7.79	8.84	4.37	662[d] (698)
Eu	197	43.1 (42.8)	4.1 (3.7)	22.6 (23.1)	2457	1635	11.00	3.48	2.83	0.35	−1.25	−2.70	0.76	1.70	730 (729)
Gd	201	42.8 (42.5)	4.0 (3.7)	22.8 (22.9)	2476 2446	1639									735 (735)
Tb	200	42.1 (42.4)	4.0 (3.7)	22.8 (22.8)	2458	1636									736 (736)
Yb	203	41.1 (41.6)	3.6 (3.6)	22.5 (22.4)	2457	1637	23.04	6.30	4.76	13.95	−11.73	−16.24	−5.30	−45.31	751 (751)
Lu	203	41.1 (41.5)	3.6 (3.6)	22.5 (22.4)	2458	1637	7.63	7.06	5.96	7.15	6.74	6.67	3.76	9.33	751 (752)

[a] As KBr disc, in some cases solid-state splitting leads to two ν(BH) values. [b] In $CDCl_3$ solution with $SiMe_4$ as internal reference. Three signals of relative areas 6:6:6 are observed from the pyrazolyl protons, in cases where coupling is resolved $^3J(HH)$ is *ca.* 2 Hz. The salicylaldehyde protons appear as four signals of relative areas 1:1:1:1 in the sal complexes and three signals of relative areas 1:1:1 in the mosal complexes which also show a singlet of area 3 due to the methoxy-methyl group. All of the complexes also show a singlet of area 1 due to the formyl proton of the bidentate ligand. [c] Most intense ion in molecular ion cluster obtained using LSIMS, calculated molecular ion values given in parentheses. [d] No molecular ion was observed, the highest-mass ion being attributable to $[M - pz]^+$.

also observed in the range 1622–1640 cm^{-1} and is attributed to the carbonyl group in the sal or mosal ligands. This shows a bathochromic shift of 28–48 cm^{-1} compared to the value found in free Hsal (1668 cm^{-1}) and is consistent with the carbonyl stretching frequency of 1620 cm^{-1} reported by Mehrotra *et al.*[10] for the homoleptic complexes $[Ln(sal)_3]$ (Ln = Y or Yb).

The electronic spectra of the new complexes (SUP 57122) contain strong absorptions which may be attributed to intraligand transitions. All of the spectra contain a band at λ_{max} 229–233 nm attributable to a π–π^* transition within the $HB(pz)_3$ ligand; additional bands, observed at 271 and 389–393 nm for the sal complexes and 426–428 nm in the mosal complexes, are attributed to transitions in the coligands.[11,12] In addition to these strong absorptions, weak Laporte-forbidden metal 4f ⟶ 4f transitions are found in the visible region. In the case of the neodymium complexes these transitions are not obscured by stronger charge-transfer absorptions and so may be used to assess the degree of covalency in the metal–ligand bonding.[13] The $4f^3$ spectra of $[Nd\{HB(pz)_3\}_2(sal)]$ and $[Nd\{HB(pz)_3\}_2(mosal)]$ are summarised in Table 2 and resemble that of the Nd^{3+} aqua ion.[14] The values of the nephelauxetic parameter, β,[13] for $[Nd\{HB(pz)_3\}_2(sal)]$ and $[Nd\{HB(pz)_3\}_2(mosal)]$ are 0.995 and 0.994, respectively. These give rise to respective values for the covalency parameter, δ,[13] of 0.49 and 0.65% indicating the effective absence of covalency in the bonding. The values of the bonding parameter, $b^{\frac{1}{2}}$[13] are also very low (respectively 0.050 and 0.057) showing that little mixing occurs between the metal 4f and ligand orbitals.

Homoleptic poly(pyrazolyl)borate complexes of the lanthanides have been evaluated as possible high-quantum-yield visible-light emitters and the emission spectra of some partially

Table 2 Visible $4f^3$ spectral data for $[Nd\{HB(pz)_3\}_2(sal)]$ and $[Nd\{HB(pz)_3\}_2(mosal)]$*

	$[Nd\{HB(pz)_3\}_2(sal)]$		$[Nd\{HB(pz)_3\}_2(mosal)]$	
Assignment	λ_{max}/nm	ε/dm^3 mol^{-1} cm^{-1}	λ_{max}/nm	ε/dm^3 mol^{-1} cm^{-1}
$^4I_{\frac{9}{2}} \longrightarrow {}^4G_{\frac{9}{2}}$	510	1.50	526	1.17
$^4I_{\frac{9}{2}} \longrightarrow {}^4G_{\frac{7}{2}}$	525	2.40	—	—
$^4I_{\frac{9}{2}} \longrightarrow {}^4G_{\frac{5}{2}}, {}^2G_{\frac{7}{2}}$	570	6.00	571	4.19
$^4I_{\frac{9}{2}} \longrightarrow {}^4G_{\frac{5}{2}}, {}^2G_{\frac{7}{2}}$	574	7.20	575	4.13
$^4I_{\frac{9}{2}} \longrightarrow {}^4G_{\frac{5}{2}}, {}^2G_{\frac{7}{2}}$	583	17.40	583	9.75
$^4I_{\frac{9}{2}} \longrightarrow {}^4F_{\frac{9}{2}}$	—	—	681	0.38
$^4I_{\frac{9}{2}} \longrightarrow {}^4F_{\frac{9}{2}}$	—	—	687	0.13
$^4I_{\frac{9}{2}} \longrightarrow {}^4S_{\frac{3}{2}}, {}^2F_{\frac{7}{2}}$	735	1.80	735	2.69
$^4I_{\frac{9}{2}} \longrightarrow {}^4S_{\frac{3}{2}}, {}^2F_{\frac{7}{2}}$	741	2.10	742	3.56
$^4I_{\frac{9}{2}} \longrightarrow {}^4S_{\frac{3}{2}}, {}^2F_{\frac{7}{2}}$	748	2.30	749	4.50
$^4I_{\frac{9}{2}} \longrightarrow {}^4S_{\frac{3}{2}}, {}^2F_{\frac{7}{2}}$	755	1.60	755	2.75
$^4I_{\frac{9}{2}} \longrightarrow {}^4H_{\frac{9}{2}}$	796	2.30	799	2.83
$^4I_{\frac{9}{2}} \longrightarrow {}^4H_{\frac{5}{2}}$	803	4.40	803	7.25
$^4I_{\frac{9}{2}} \longrightarrow {}^4H_{\frac{5}{2}}$	811	sh	811	2.38
$^4I_{\frac{9}{2}} \longrightarrow {}^4F_{\frac{3}{2}}$	861	0.75	861	1.13
$^4I_{\frac{9}{2}} \longrightarrow {}^4F_{\frac{3}{2}}$	877	0.90	877	0.94

* Obtained from 0.04 mol dm^{-3} solutions in CH_2Cl_2.

characterised europium and terbium poly(pyrazolyl)borate complexes have been reported.[15] A ligand-to-metal charge-transfer (l.m.c.t.) process, present only in the complex, was thought to lead to population of the lanthanide excited state according to the Whan–Crosby mechanism.[16] The heteroleptic europium and terbium complexes reported here are also luminescent and their emission spectra are summarised in Table 3. Excitation of either the europium or the terbium complexes at a wavelength of 230–233 nm results in emission, that from the terbium complexes being the more intense. In the case of europium four emission bands are resolved corresponding to the transitions from the $^5D_0$ excited state to the ^7F_J (J = 1–4) levels. The emission spectra of the terbium complexes similarly contain four bands corresponding to the transitions from the $^5D_4$ excited state to the ^7F_J (J = 3–6) levels.[17] Similar but more intense emission spectra were recorded from $[Ln\{HB(pz)_3\}_2(sal)]$ (Ln = Eu or Tb) on excitation of the coligand absorption at 271–272 nm. Since the molar absorption coefficient of this absorption is less than half that associated with the tris(pyrazolyl)borate ligand, it would appear that energy transfer to the lanthanide ion is more efficient from the salicylaldehyde coligand than from the tris(pyrazolyl)borate ligand in these complexes. Excitation at 391 nm gave observable emission only in the case of the Eu^{3+} complex in which the emissive $^5D_0$ level lies at lower energy than the $^5D_4$ level of Tb^{3+}.[17] Excitation of the complexes $[Ln\{HB(pz)_3\}_2(mosal)]$ (Ln = Eu or Tb) at 426–428 nm did not lead to any observed emission and it seems that, in these complexes, the coligand excited state is insufficiently energetic to effect energy transfer to the emissive states of either lanthanide ion. In favourable circumstances structural information may be obtained from such emission spectra and $[Tb\{H_2B(pz)_2\}_3]$ has been shown to have C_3 symmetry by this method.[18] However, no ligand-field splitting could be resolved in the $^5D_0 \longrightarrow {}^7F_J$ or $^5D_4 \longrightarrow {}^7F_J$ bands of the Eu^{3+} (J = 1–4) or Tb^{3+} (J = 3–6) complexes so that information on their structures in solution could not be obtained.

The ^1H NMR spectra (Table 1) of the diamagnetic complexes containing Y^{3+} or Lu^{3+} ions exhibit three signals, each of relative area 6, attributable to the $HB(pz)_3$ protons. This observation is consistent with rapid intramolecular ligand reorganisation as found in other complexes of this type[6–8] but not in $[Y\{HB(pz)_3\}_3]$.[19] In the complexes containing sal, signals are also observed for the single aldehyde and four aryl protons. For the mosal complexes four signals of relative area 1 are observed as well as one of relative area 3 from the methoxy methyl protons. The paramagnetic complexes reveal similar patterns but these are shifted by the proximity of the paramagnetic centres as observed in other examples of complexes of this type.[6,7,20] The respective magnetic moments of the gadolinium complexes $[Gd\{HB(pz)_3\}_2(sal)]$ and $[Gd\{HB(pz)_3\}_2(mosal)]$ were found to be 7.91 and 7.77 μ_B, close to the spin-only value of 7.94 μ_B for an f^7 system, and to the value of 7.84 μ_B found for $[Gd\{HB(pz)_3\}_3]$.

Structural studies

The complex $[Eu\{HB(pz)_3\}_2(mosal)]$ crystallises from CH_2Cl_2–hexane solution to form air-stable, orange, monoclinic, plates of space group $P2_1/n$ ($P2_1/c$). Fractional atomic coordinates are listed in Table 4 and selected geometrical parameters in Table 5. The molecular structure is illustrated in Fig. 1 which also shows the numbering scheme. All pyrazolyl rings are labelled similarly.

The crystal structure consists of discrete monomeric molecular units, as found with other $[Ln\{HB(pz)_3\}_2X]$ (Ln = Ce or Yb, X = acac; Ln = Yb, X = $O_2C_7H_5$ or O_2CPh) complexes. The europium ion is eight-co-ordinate, and both of the borate ligands are tridentate. The mosal ligand is bidentate through the phenolate and aldehyde functionalities. The geometry of the N_6O_2 co-ordination sphere may be related to the three regular co-ordination geometries [square antiprismatic (*SAPR*), C_{2v} bicapped trigonal prismatic (*TPRB*) and dodecahedral (*DD*)] using the semiquantitative method of polytopal analysis[22] and values for δ and φ are presented in Table 6. The structure of the molecule resembles that of $[Ce\{HB(pz)_3\}_2(acac)]$,[6] except that there is some twisting of one of the borate ligands. However, whilst the co-ordination geometry of $[Ce\{HB(pz)_3\}_2(acac)]$ is best described as *TPRB*, this is not true for $[Eu\{HB(pz)_3\}_2(mosal)]$ which is basically *DD*, as shown in Fig. 2.

The shortest europium-to-ligand bond lengths are to the oxygen atoms, of which the bond to the phenolate oxygen is the shorter at 2.266(5) Å. This value is fairly typical of the limited number of other europium phenolate structures reported so far; for example, the Eu–O (phenolate) distances in the disordered $[Eu_2(HA)_2(dmf)_4]\cdot 7dmf$ (H_4A = *p-tert*-butylcalix[4]arene, dmf = dimethylformamide)[23] range between 2.143(6) and 2.395(6), mean 2.255(3) Å. The longer Eu–O distance of 2.402(5) Å to the oxygen of the CHO group corresponds to europium–carbonyl (dmf) bond distances in $[Eu(H_4E)(dmf)_6(OH)]\cdot H_6E\cdot \approx 4dmf$ (H_6E = *p-tert*-butylcalix[6]arene),[24] which average 2.434(9) Å. The difference in bond lengths from the Eu atom to the two oxygen atoms in $[Eu\{HB(pz)_3\}_2(mosal)]$

Table 3 Emission spectral data for $[Ln\{HB(pz)_3\}_2X]$ (Ln = Eu or Tb; X = sal or mosal)[a]

Complex	λ/nm Excitation	Emission	Assignment	Measured intensity[b]	Relative intensity[c] (%)
$[Eu\{HB(pz)_3\}_2(sal)]$	233	593	$^5D_0 \longrightarrow {}^7F_1$	1.1	41
		615	$^5D_0 \longrightarrow {}^7F_2$	2.8	100
		654	$^5D_0 \longrightarrow {}^7F_3$	1.0	35
		698	$^5D_0 \longrightarrow {}^7F_4$	2.0	72
$[Eu\{HB(pz)_3\}_2(sal)]$	272	591	$^5D_0 \longrightarrow {}^7F_1$	166	38
		615	$^5D_0 \longrightarrow {}^7F_2$	434	100
		652	$^5D_0 \longrightarrow {}^7F_3$	46	11
		699	$^5D_0 \longrightarrow {}^7F_4$	288	66
$[Eu\{HB(pz)_3\}_2(sal)]$	391	589	$^5D_0 \longrightarrow {}^7F_1$	23	41
		616	$^5D_0 \longrightarrow {}^7F_2$	55	100
		651	$^5D_0 \longrightarrow {}^7F_3$	5.0	9
		698	$^5D_0 \longrightarrow {}^7F_4$	19	34
$[Tb\{HB(pz)_3\}_2(sal)]$	231	490	$^5D_4 \longrightarrow {}^7F_6$	72	40
		544	$^5D_4 \longrightarrow {}^7F_5$	179	100
		586	$^5D_4 \longrightarrow {}^7F_4$	50	28
		621	$^5D_4 \longrightarrow {}^7F_3$	26	15
$[Tb\{HB(pz)_3\}_2(sal)]$	271	490	$^5D_4 \longrightarrow {}^7F_6$	249	48
		544	$^5D_4 \longrightarrow {}^7F_5$	519	100
		586	$^5D_4 \longrightarrow {}^7F_4$	120	23
		620	$^5D_4 \longrightarrow {}^7F_3$	77	15
$[Tb\{HB(pz)_3\}_2(sal)]$[d]	390				
$[Eu\{HB(pz)_3\}_2(mosal)]$	230	591	$^5D_0 \longrightarrow {}^7F_1$	3.1	64
		616	$^5D_0 \longrightarrow {}^7F_2$	4.8	100
		651	$^5D_0 \longrightarrow {}^7F_3$	1.5	30
		699	$^5D_0 \longrightarrow {}^7F_4$	3.3	68
$[Tb\{HB(pz)_3\}_2(mosal)]$	231	492	$^5D_4 \longrightarrow {}^7F_6$	50	44
		544	$^5D_4 \longrightarrow {}^7F_5$	114	100
		586	$^5D_4 \longrightarrow {}^7F_4$	32	28
		620	$^5D_4 \longrightarrow {}^7F_3$	17	15
$[Eu\{HB(pz)_3\}_2(mosal)]$[d]	426				
$[Tb\{HB(pz)_3\}_2(mosal)]$[d]	428				

[a] Obtained from 10^{-4} (europium complexes) or 10^{-5} mol dm^{-3} (terbium complexes) solutions in CH_2Cl_2. [b] Reported in arbitrary units in which the weakest emission of the series (*i.e.* for $[Eu\{HB(pz)_3\}_2(sal)]$, $^5D_0 \longrightarrow {}^7F_3$) is set at unity. [c] Relative to the strongest emission (set at 100%) for the complex at the specified excitation wavelength. [d] No observed emission.

Table 4 Atomic coordinates ($\times 10^4$) for $[Eu\{HB(pz)_3\}_2(mosal)]$

Atom	*x*	*y*	*z*	Atom	*x*	*y*	*z*
Eu	404(1)	1180(1)	3053(1)	C(31)	−3727(8)	1456(3)	2378(6)
N(11)	889(6)	1444(2)	1101(4)	C(32)	−4735(8)	1788(3)	1956(6)
N(12)	342(6)	1832(2)	692(4)	C(33)	−3731(8)	2086(3)	1526(6)
N(21)	1299(6)	1981(2)	3064(4)	C(41)	−1716(9)	1992(2)	4565(6)
N(22)	494(6)	2282(2)	2394(4)	C(42)	−1957(8)	2131(2)	5595(6)
N(31)	−2167(6)	1541(2)	2213(4)	C(43)	−1372(8)	1799(2)	6253(5)
N(32)	−2182(6)	1933(2)	1677(4)	C(51)	3949(8)	1154(3)	4924(6)
N(41)	−1011(7)	1596(2)	4574(4)	C(52)	4493(10)	1088(3)	5986(7)
N(42)	−811(6)	1477(2)	5639(4)	C(53)	3118(10)	1024(3)	6503(6)
N(51)	2309(6)	1138(2)	4792(4)	C(61)	−1847(8)	276(3)	3982(6)
N(52)	1805(7)	1058(2)	5778(4)	C(62)	−2443(9)	92(3)	4891(7)
N(61)	−916(6)	628(2)	4238(4)	C(63)	−1812(9)	348(3)	5728(7)
N(62)	−892(6)	667(2)	5337(4)	C(1)	31(11)	240(3)	1536(6)
O(1)	2616(7)	792(2)	2615(4)	C(2)	1632(10)	141(3)	1645(5)
O(2)	−564(8)	579(2)	1911(4)	C(3)	2091(13)	−298(3)	1165(6)
O(3)	4270(8)	−795(2)	860(6)	C(4)	3628(13)	−411(3)	1220(7)
C(11)	1683(9)	1251(3)	332(5)	C(5)	4827(15)	−125(3)	1707(9)
C(12)	1668(10)	1516(3)	−572(6)	C(6)	4494(12)	270(4)	2172(9)
C(13)	815(9)	1881(3)	−316(5)	C(7)	2889(9)	395(3)	2123(6)
C(21)	2092(8)	2213(2)	3856(5)	C(8)	3245(14)	−1090(4)	341(9)
C(22)	1801(9)	2656(3)	3712(6)	B(1)	−598(8)	2148(3)	1360(5)
C(23)	781(8)	2686(2)	2775(5)	B(2)	8(10)	1044(3)	5993(6)

thus reflects the presence of a negative charge on the phenolate functionality. The longest Eu–N bond lengths are those to N(11) and N(41), at 2.606(5) and 2.618(5) Å. Interestingly, these atoms are the 'capping' atoms if the geometry is considered to be derived from that of $[Ce\{HB(pz)_3\}_2(acac)]$. In other complexes containing the $Ln[HB(pz)_3]_2^+$ moiety where there is an element of *TPRB* geometry in the co-ordination polyhedron the bonds to 'capping' atoms are usually longer than those to comparable non-capping atoms.[6,7,19] The other Eu–N distances range from 2.533(5) to 2.547(5) Å except for Eu–N(31) which is 2.515(5) Å. If the 'geometric pathway' from $[Ce\{HB(pz)_3\}_2(acac)]$ to the more sterically congested $[Yb\{HB(pz)_3\}_2(acac)]$ involves a concerted 'slippage' of both borate ligands with respect to the third ligand, then the distortion in $[Eu\{HB(pz)_3\}_2(mosal)]$, which is intermediate in steric congestion, is equivalent to the slippage of only one borate ligand, namely that containing N(41), N(51) and N(61). The pyrazolyl ring containing N(31) is immediately adjacent to

Table 5 Selected bond lengths (Å) and angles (°) for [Eu{HB(pz)$_3$}$_2$(mosal)]

Eu–O(1)	2.266(5)	O(3)–C(8)	1.352(11)
Eu–O(2)	2.402(5)	O(3)–C(4)	1.370(10)
Eu–N(31)	2.515(5)	C(1)–C(2)	1.340(11)
Eu–N(61)	2.533(5)	C(2)–C(7)	1.377(11)
Eu–N(21)	2.543(5)	C(2)–C(3)	1.521(11)
Eu–N(51)	2.547(5)	C(3)–C(4)	1.301(12)
Eu–N(11)	2.606(5)	C(4)–C(5)	1.407(13)
Eu–N(41)	2.618(5)	C(5)–C(6)	1.368(13)
O(1)–C(7)	1.379(9)	C(6)–C(7)	1.364(11)
O(2)–C(1)	1.246(10)		
O(1)–Eu–O(2)	72.1(2)	O(2)–Eu–N(41)	130.2(2)
O(1)–Eu–N(31)	141.7(2)	N(31)–Eu–N(41)	71.3(2)
O(2)–Eu–N(31)	82.4(2)	N(61)–Eu–N(41)	70.5(2)
O(1)–Eu–N(61)	100.5(2)	N(21)–Eu–N(41)	71.3(2)
O(2)–Eu–N(61)	72.5(2)	N(51)–Eu–N(41)	72.2(2)
N(31)–Eu–N(61)	98.3(2)	N(11)–Eu–N(41)	129.0(2)
O(1)–Eu–N(21)	105.4(2)	C(7)–O(1)–Eu	136.5(5)
O(2)–Eu–N(21)	144.3(2)	C(1)–O(2)–Eu	136.8(6)
N(31)–Eu–N(21)	79.3(2)	C(8)–O(3)–C(4)	118.7(8)
N(61)–Eu–N(21)	140.3(2)	O(2)–C(1)–C(2)	124.0(9)
O(1)–Eu–N(51)	74.5(2)	C(1)–C(2)–C(7)	127.1(8)
O(2)–Eu–N(51)	127.2(2)	C(1)–C(2)–C(3)	115.5(8)
N(31)–Eu–N(51)	143.0(2)	C(7)–C(2)–C(3)	117.4(8)
N(61)–Eu–N(51)	74.9(2)	C(4)–C(3)–C(2)	118.8(9)
N(21)–Eu–N(51)	83.6(2)	C(3)–C(4)–O(3)	127.2(10)
O(1)–Eu–N(11)	75.5(2)	C(3)–C(4)–C(5)	119.6(9)
O(2)–Eu–N(11)	76.0(2)	O(3)–C(4)–C(5)	113.2(9)
N(31)–Eu–N(11)	70.9(2)	C(6)–C(5)–C(4)	124.4(11)
N(61)–Eu–N(11)	147.9(2)	C(7)–C(6)–C(5)	116.9(10)
N(21)–Eu–N(11)	69.1(2)	C(6)–C(7)–C(2)	122.8(9)
N(51)–Eu–N(11)	131.8(2)	C(6)–C(7)–O(1)	114.7(8)
O(1)–Eu–N(41)	146.7(2)	C(2)–C(7)–O(1)	122.5(7)

the putative vacancy caused by slippage, and the apparent slight contraction in this bond distance may be attributable thereto.

Polytopal analysis is a method of assessing the conformity of the co-ordination polyhedron formed by the ligating atoms to certain ideal polyhedra, by means of comparing diagnostic internal angles. Table 6 contains δ and φ values for [{Sm[HB(pz)$_3$]$_2$(O$_2$CPh)}$_2$],[9] which has not previously been examined in this way, and [Eu{HB(pz)$_3$}$_2$(mosal)] for comparison. The values are presented for both the actual polyhedra and the normalised polyhedra, in which 'anomalies' due to shorter Ln–O bonds, *etc.* are removed by setting all metal-to-ligand bond distances to 1 Å.[22] The values for [Eu{HB(pz)$_3$}$_2$(mosal)] suggest that the polyhedron geometry is best described as *DD*. The major source of distortion in both the normalised and unnormalised polyhedra is the constraint placed upon the N(21)···N(31) (non-bonded) distance. This corresponds to one of the 'equatorial' distances (*i.e.* one of the four long edges of an eight-vertex dodecahedron) of a 'hard-sphere' model[18] and might thus be expected to be 1.5 Å in a normalised dodecahedron. This is evidently an unreasonable constraint to place upon the borate ligand and the N(21)···N(31) distance is consequently 1.277(7) Å in the normalised co-ordination polyhedron. Otherwise the dodecahedral geometry is relatively undistorted, the other three 'equatorial' bonds averaging 1.547(4) Å and fourteen 'non-equatorial' distances averaging 1.204(2) Å (theoretical value 1.2 Å). In [{Sm[HB(pz)$_3$]$_2$(O$_2$CPh)}$_2$][10] one metal centre [Sm(1)] is distorted beyond description by the polytopal analysis method but values for Sm(2) indicate a *DD* geometry.

The electronic spectral data described above for [Nd{HB(pz)$_3$}$_2$(mosal)] and [Nd{HB(pz)$_3$}$_2$(mosal)] are consistent with highly ionic bonding, indicating that it is appropriate to discuss the structures of these complexes in terms of steric angle sum values. Accordingly we have sought to use such calculations to explain why, with the mosal ligand, Eu^{3+} forms monomeric [Eu{HB(pz)$_3$}$_2$(mosal)] whilst, with benzoate, the similarly

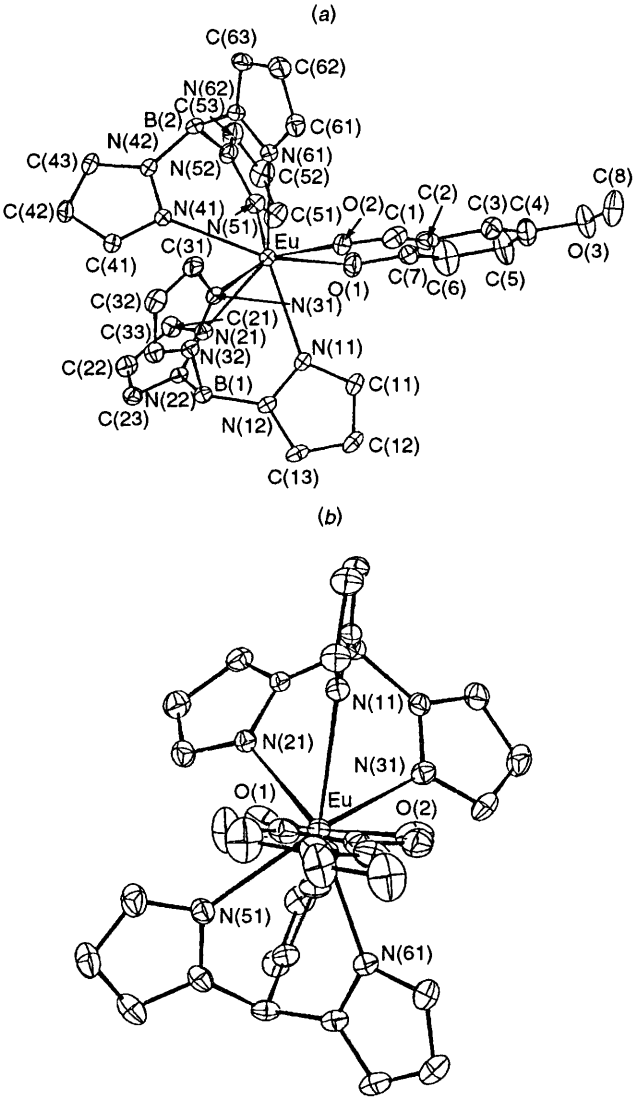

Fig. 1 Views of the [Eu{HB(pz)$_3$}$_2$(mosal)] molecule showing the atom labelling. Hydrogen atoms are omitted for clarity. The plotting routine used was SNOOPI:[21] (*a*) general; (*b*) along the O(3)–C(4) axis showing the relative orientations of the borate ligands

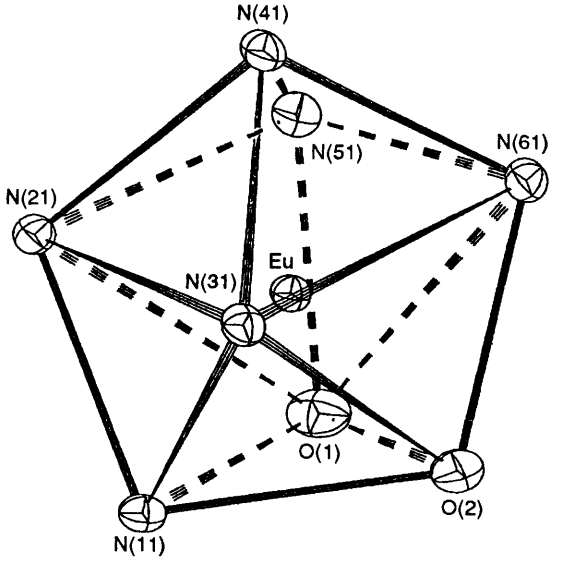

Fig. 2 The co-ordination geometry around the Eu atom in [Eu{HB(pz)$_3$}$_2$(mosal)] plotted by SNOOPI[21]

Table 6 Values of δ and φ/° for [Eu{HB(pz)$_3$}$_2$(mosal)] and [{Sm[HB(pz)$_3$]$_2$(O$_2$CPh)}$_2$]

[Eu{HB(pz)$_3$}$_2$(mosal)]			[{Sm[HB(pz)$_3$]$_2$(O$_2$CPh)}$_2$]							
	Around Eu			Around Sm(1)		Around Sm(2)		Idealised polyhedra		
Atoms	P[a]	NP[a]	Atoms	P[a]	NP[a]	P[a]	NP[a]	DD	SAPR	TPRB
N(41)[N(61)N(31)]O(2)	δ 29.5	29.2	1(57)3[b]	δ 39.1	42.9	22.9	23.7	29.5	0.0	21.8
N(51)[N(21)O(1)]N(11)	δ 19.0	24.3	2(68)4	δ 32.1	33.6	35.7	39.5	29.5	0.0	0.0
N(51)[N(61)O(1)]O(2)	δ 21.9	24.5	2(58)3	δ 20.1	19.4	29.3	33.0	29.5	52.5	48.2
N(41)[N(21)N(31)]N(11)	δ 38.5	41.2	1(67)4	δ 11.0	16.6	22.5	23.2	29.5	52.5	48.2
N(31)–N(41)–N(51)–O(1)	φ 4.2	4.2	7–1–2–8	φ 10.8	11.3	3.2	3.5	0.0	24.5	14.1
N(61)–O(2)–N(11)–N(21)	φ 0.5	0.9	5–3–4–6	φ 7.1	7.0	1.2	1.2	0.0	24.5	14.1

[a] P = Actual co-ordination polyhedron, NP = normalised polyhedron. [b] Polyhedral vertices defined as: 1 [N(62), O(4)], 2 [O(1), N(72)], 3 [N(32), N(112)], 4 [N(22), N(102)], 5 [N(52), O(2)], 6 [O(3), N(92)], 7 [N(42), N(122)] and 8 [N(12), N(82)].

sized Sm^{3+} ion forms dimeric [{Sm[HB(pz)$_3$]$_2$(O$_2$CPh)}$_2$]. It is known that the IR spectrum of [Y{HB(pz)$_3$}$_2$(O$_2$CMe)] is dependent upon the solvent from which crystallisation takes place,[7,25] but our attempts to produce monomeric [Sm{HB(pz)$_3$}$_2$(O$_2$CPh)] by crystallisation from CH_2Cl_2–hexane mixtures, as used to crystallise [Eu{HB(pz)$_3$}$_2$(mosal)], afforded only crystals of reported dimeric morphology.[9] The s.a.s. value for monomeric [Eu{HB(pz)$_3$}$_2$(mosal)] is 0.768, which consists of a contribution of 0.200 from the mosal ligand and an average of 0.284 from each borate ligand (any discrepancy between the sum of these s.a.f. values and the s.a.s. is due to a correction applied for van der Waals interligand overlap of the ligating atoms).[2] Dimeric [{Sm[HB(pz)$_3$]$_2$(O$_2$CPh)}$_2$] has two metal centres, and thus has two ascribable s.a.s. values. Atom Sm(1) has an s.a.s. value of 0.787, attributable to a contribution of 0.205 from the 'metallaligand' and an average of 0.292 from borate ligands. The corresponding values for Sm(2) are 0.776, 0.195 and 0.292. The value for [Eu{HB(pz)$_3$}$_2$(mosal)] makes it typical of an eight-co-ordinate complex, and those for [{Sm[HB(pz)$_3$]$_2$(O$_2$CPh)}$_2$] are within half a standard deviation of the mean for this class.[2] As might be expected, the s.a.s. values for [Eu{HB(pz)$_3$}$_2$(mosal)] and [{Sm[HB(pz)$_3$]$_2$(O$_2$CPh)}$_2$] fall between the extremes represented by [Ce{HB(pz)$_3$}$_2$(acac)] on the one hand and the [Yb{HB(pz)$_3$}$_2$X] complexes on the other, as do the s.a.f. values for the borate ligands in these structures. This is in keeping with the expected effects of the decreasing ionic radii of the lanthanides across the series.

A crude estimate of the expected s.a.s. value of monomeric [Sm{HB(pz)$_3$}$_2$(O$_2$CPh)] can be made by assuming a symmetrically bound benzoate ligand with a bite distance equal to the mean intraligand O···O distance in [{Sm[HB(pz)$_3$]$_2$(O$_2$CPh)}$_2$]. If the Sm–O distance is set equal to the mean found in this dimer the s.a.s. value of the monomer is estimated to be 0.764 and less than the values found in the structure of the dimer and the mean value for eight co-ordinate complexes of 0.78 mentioned earlier.[2] Thus it seems that in the dimer the intermediately sized Sm^{3+} ion can achieve a larger s.a.s. value than would be expected for monomeric [Sm{HB(pz)$_3$}$_2$(O$_2$CPh)], providing a driving force for dimerisation. The failure of [Eu{HB(pz)$_3$}$_2$(mosal)] to dimerise, despite having an s.a.s. almost equal to that estimated for the monomeric samarium complex, may be due to the greater steric demands of the salicylaldehyde group, compared to benzoate, in the secondary co-ordination sphere.

Applying a reversal of the above extrapolation to [Yb{HB(pz)$_3$}$_2$(O$_2$CPh)] leads to the conclusion that, if this complex were to exist as a benzoate-bridged dimer, its s.a.s. value may be estimated as 0.834, larger than that of [Yb{HB(pz)$_3$}$_2$(acac)] and well above the mean of 0.78.[2] Since the observed[7] monomeric structure for [Yb{HB(pz)$_3$}$_2$(O$_2$CPh)] gives an s.a.s. value of 0.814, closer to the mean, it may be that in this case, dimerisation leads to a sterically oversaturated structure.

Although the errors in estimating s.a.s. values, and the relatively wide range of values found experimentally, limit their application, this approach does provide a useful framework for comparing the structures of heteroleptic lanthanide complexes. However, the similarity between the observed s.a.s. value of [Eu{HB(pz)$_3$}$_2$(mosal)] and that estimated for [Sm{HB(pz)$_3$}$_2$(O$_2$CPh)], which dimerised, illustrates the need for caution in using s.a.s. calculations in an absolute or predictive manner.

Experimental

Syntheses and spectroscopy

Potassium hydrotris(pyrazol-1-yl)borate was prepared by the literature method.[25] Hydrated lanthanide trichlorides were obtained from Ventron GMBH, salicylaldehyde and 5-methoxysalicylaldehyde from Aldrich Chemicals Ltd. The former was redistilled before use and the latter used without further purification.

Infrared spectra were recorded on Perkin-Elmer 297 or 1600 spectrometers using potassium bromide pellets, UV/VIS spectra using a Shimadzu UV240 spectrometer and emission spectra using a Spexfluorolog spectrofluorimeter and data station. Room-temperature magnetic susceptibility measurements were made using a Johnson Matthey susceptibility balance with Hg[Co(SCN)$_4$] as the calibrant. The EPR spectra were measured at 298 K using a Bruker ESP300 spectrometer, ^{1}H NMR spectra using JEOL JNM GX270 and Bruker WH300 spectrometers. Deuteriated NMR solvents were obtained from Aldrich Chemicals Ltd., and chemical shifts are reported with tetramethylsilane as internal reference at 293 K. Mass spectra were obtained using a Kratos MS80RF mass spectrometer, ions being produced by fast argon-atom bombardment or electron impact.

[Ln{HB(pz)$_3$}$_2$(sal)], general procedure. A solution of K[HB(pz)$_3$] (0.50 g, 2 mmol) and salicylaldehyde (0.12 g, 1 mmol) in ethanol (10 cm^3) was mixed with an aqueous solution (10 cm^3) of KOH (0.1 mol dm^{-3}), then added to a solution of the appropriate lanthanide (or yttrium) trichloride hydrate (1 mmol) in water (15 cm^3). The resulting mixture was stirred for 15 min and the precipitate which formed was filtered off and dried at 100 °C overnight. The crude product was dissolved in dichloromethane (*ca.* 10 cm^3), the solution filtered and a similar volume of hexane added. Slow evaporation led to deposition of crystals of the product. Yields and characterisation data are presented in Table 1.

[Ln{HB(pz)$_3$}$_2$(mosal)], general procedure. A solution of K[HB(pz)$_3$] (0.50 g, 2 mmol) and 5-methoxysalicylaldehyde

(0.15 g, 1 mmol) in ethanol (10 cm^3) was mixed with an aqueous solution of KOH (10 cm^3, 0.1 mol dm^{-3}) then added to a solution of the appropriate yttrium or lanthanide trichloride hydrate (1 mmol) in water (15 cm^3). The resulting mixture was stirred for 15 min and the precipitate which formed was filtered off and dried at 100 °C overnight. The crude product was dissolved in dichloromethane (*ca.* 10 cm^3), the solution filtered and a similar volume of hexane added. Slow evaporation led to deposition of crystals of the product.

Crystallography

Crystal data for [Eu{HB(pz)$_3$}$_2$(mosal)]. $C_{25}H_{27}B_2EuN_{12}O_3$, $M = 717.2$, monoclinic, space group $P2_1/n$ [non-standard setting of $P2_1/c$ (no. 14)], $a = 8.184(1)$, $b = 30.410(9)$, $c = 12.367(2)$ Å, $\beta = 95.01(1)°$, $U = 3065.9$ Å^3, $Z = 4$, $D_c = 1.58$ g cm^{-3}, Mo-Kα radiation ($\lambda = 0.710\,69$ Å), $\mu = 2.10$ mm^{-1}, $T = 293$ K.

Data were collected on an Enraf-Nonius CAD4 diffractometer at the Crystallography Unit, Universities of Aston and Birmingham. Accurate unit-cell dimensions were obtained from the setting angles of 25 reflections with $12 < \theta < 16°$ (chosen from the final data set). Intensities were measured with an ω–2θ scan method in bisecting geometry, a variable scan rate and ω-scan angle of $(1.00 + 0.35 \tan \theta)°$. 6981 Reflections were measured with $2 < \theta < 25°$, $-1 < h < 9$, $-1 < k < 36$ and $-14 < l < 14$. Two standard reflections were measured every hour during data collection and showed little variation with time. Data were corrected for Lorentz and polarisation effects, and adjusted for slight standard decay. The europium atom position was estimated using Patterson[27] techniques, whereafter equivalent reflections were merged to give 5357 unique data with $I > 0$. The remaining non-hydrogen atom positions were estimated from subsequent Fourier-difference syntheses and the resulting model refined by full-matrix least-squares methods using program default[28] values for scattering factors and anomalous dispersion terms for all atoms. Hydrogens were fixed in calculated default[28] positions with a common refined isotropic thermal parameter. An absorption correction,[29] based upon the best full model containing anisotropic non-H atoms, was applied (maximum 1.148, minimum 0.881). Convergence was considered complete when the final shift in any parameter was less than 0.01 of the e.s.d. thereof, whereupon the equivalent[28] conventional R value was 0.0424 for 4223 data with $I > 2\sigma(I)$ and $wR2$ was[28] 0.0989 at convergence. The largest peak in the final difference map was 1.13 e Å^{-3}, at 0.97 Å from O(1). No unusually close intermolecular contacts were found.

Complete atomic coordinates, thermal parameters and bond lengths and angles have been deposited at the Cambridge Crystallographic Data Centre. See Instructions for Authors, *J. Chem. Soc., Dalton Trans.*, 1996, Issue 1.

Acknowledgements

We are grateful to Dr. T. A. Hamor and The Universities of Aston and Birmingham Crystallography Unit for the provision of crystallography facilities and to the SERC (now EPSRC) and Zeneca Specialties for support (to R. G. L.) through the CASE scheme.

References

1 T. Moeller, *The Chemistry of the Lanthanides*, Reinhold, New York, 1963.
2 Feng Xi-zhang, Guo Ao-ling, Xu Ying-ting, Li Xing-fu and Sun Peng-nian, *Polyhedron*, 1987, **6**, 1041.
3 K. W. Bagnall, A. C. Tempest, J. Takats and A. P. Masino, *Inorg. Nucl. Chem. Lett.*, 1976, **12**, 555.
4 M. A. J. Moss and C. J. Jones, *Abstracts of the XXIV International Conference on Coordination Chemistry*, Chimika Chronika, Association of Greek Chemists, 1986, A7-488.
5 W. D. Moffat, M. V. R. Stainer and J. Takats, *Inorg. Chim. Acta*, 1987, **139**, 75.
6 M. A. J. Moss, C. J. Jones and A. J. Edwards, *J. Chem. Soc., Dalton Trans.*, 1989, 1393.
7 M. A. J. Moss and C. J. Jones, *J. Chem. Soc., Dalton Trans.*, 1990, 581.
8 M. A. J. Moss and C. J. Jones, *Polyhedron*, 1990, **9**, 697.
9 D. L. Reger, S. J. Knox, J. A. Lindeman and L. Lebioda, *Inorg. Chem.*, 1990, **29**, 416.
10 R. C. Mehrota, P. N. Kapoor and J. M. Batwara, *Coord. Chem. Rev.*, 1980, **31**, 67.
11 K. K. Rohatgi and S. K. Sen Gupta, *J. Inorg. Nucl. Chem.*, 1972, **34**, 3061.
12 R. A. Morton and A. L. Stubbs, *J. Chem. Soc.*, 1940, 1347.
13 S. N. Misra and S. O. Sommerer, *Appl. Spectrosc. Rev.*, 1991, **26**, 151; M. Mohan, J. P. Tandon and N. S. Gupta, *Inorg. Chim. Acta*, 1986, **111**, 187.
14 K. B. Yatsmirskii and N. K. Davidenko, *Coord. Chem. Rev.*, 1979, **27**, 223.
15 R. A. Faltynek, *J. Coord. Chem.*, 1989, **20**, 73.
16 R. E. Whan and G. A. Crosby, *J. Mol. Spectrosc.*, 1962, **8**, 315.
17 (*a*) G. E. Buono-Core and H. Li, *Coord. Chem. Rev.*, 1990, **99**, 55; (*b*) F. A. Hart, in *Comprehensive Coordination Chemistry*, eds. G. Wilkinson, R. D. Gillard and J. A. McCleverty, 1987, vol. 3, ch. 39, pp. 1105–1109; (*c*) F. S. Richarson, *Chem. Rev.*, 1982, **82**, 541.
18 D. L. Reger, P. T. Chou, S. L. Studer, S. J. Knox, M. L. Martinez, and W. E. Brewer, *Inorg. Chem.*, 1991, **30**, 2397.
19 M. V. R. Stainer and J. Takats, *J. Am. Chem. Soc.*, 1983, **105**, 410.
20 Ref. 17(*b*), pp. 1100–1105.
21 E. K. Davies, SNOOPI, Chemical Crystallography Laboratory, University of Oxford, 1982.
22 M. A. Porai-Koshits and L. A. Aslanov, *J. Struct. Chem.*, 1978, **13**, 244; M. G. B. Drew, *Coord. Chem. Rev.*, 1977, **24**, 179.
23 B. M. Furphy, J. MacB. Harrowfield, M. I. Ogden, B. W. Skelton, A. H. White and F. R. Wilner, *J. Chem. Soc., Dalton Trans.*, 1989, 2217.
24 L. M. Engelhardt, B. M. Furphy, J. MacB. Harrowfield, D. L. Kepert, A. H. White and F. R. Wilner, *Aust. J. Chem.*, 1988, **41**, 1465.
25 D. L. Reger, J. A. Lindeman and L. Lebioda, *Inorg. Chem.*, 1988, **27**, 3923.
26 S. Trofimenko, *Inorg. Synth.*, 1970, **12**, 99.
27 G. M. Sheldrick, SHELXS 86, Program for the Solution of Crystal Structures, University of Göttingen, 1976.
28 G. M. Sheldrick, SHELXL 93, Program for Crystal Structure Refinement, University of Göttingen, 1993.
29 N. Walker and D. Stuart, *Acta Crystallogr., Sect. A*, 1983, **39**, 158.

Received 9th June 1995; *Paper* 5/03717D